

PHYSICS WITH THE STAR DETECTOR AT RHIC

T. J. LeCOMPTE

High Energy Physics Division

Argonne National Laboratory

9700 S. Cass Avenue Argonne, IL 60439

E-mail: lecompte@anl.gov

(for the STAR Collaboration)

I discuss the capabilities of the STAR detector at RHIC and a subset of the physics program the STAR collaboration hopes to undertake with this detector.

1 Introduction

The Relativistic Heavy Ion Collider (RHIC) at Brookhaven National Laboratory will collide beams of nuclei (as light as protons and as heavy as gold) at energies of up to 200 GeV per nucleon. At these energies, the probability of detecting a phase transition to a state of matter where quarks and gluons are not confined to nucleons is large. (The nuclear densities are approaching nucleon densities) Additionally, the collision is occurring in a kinematic regime where perturbative QCD is expected to be reliable.

The STAR (Solenoidal Detector at RHIC) detector is designed to study pp , pA and AA collisions at RHIC. It is a 4π detector emphasizing the detection and measurement of hadrons. The philosophy of the detector design is to measure many quantities of interest per event, so that events can be categorized and correlated based on these characteristics. Nobody knows for sure what a Quark-Gluon Plasma looks like, so STAR was designed with a broad range of potential measurements in mind, to maximize the discovery potential.

This paper is not intended to give a complete description of all of the physics measurements the STAR collaboration intends to do. Such a description is not possible within the space constraints. However, it is intended to give the reader a flavor of the capabilities of the detector and the kinds of measurements that are possible at STAR.

2 Detector

As mentioned before, the STAR detector is a 4π experiment emphasizing the detection and measurement of hadrons. It is designed around a 0.5 Tesla conventional solenoidal magnet. Inside the magnet are detectors for tracking

* Work supported in part by the U.S. Department of Energy,
Division of High Energy Physics, Contract W-31-109-ENG-38.

The submitted manuscript has been created by the University of Chicago as Operator of Argonne National Laboratory ("Argonne") under Contract No. W-31-109-ENG-38 with the U.S. Department of Energy. The U.S. Government retains for itself, and others acting on its behalf, a paid-up, nonexclusive, irrevocable worldwide license in said article to reproduce, prepare derivative works, distribute copies to the public, and perform publicly and display publicly, by or on behalf of the Government.

RECEIVED
OSTI
SEP 28 1998

DISCLAIMER

This report was prepared as an account of work sponsored by an agency of the United States Government. Neither the United States Government nor any agency thereof, nor any of their employees, make any warranty, express or implied, or assumes any legal liability or responsibility for the accuracy, completeness, or usefulness of any information, apparatus, product, or process disclosed, or represents that its use would not infringe privately owned rights. Reference herein to any specific commercial product, process, or service by trade name, trademark, manufacturer, or otherwise does not necessarily constitute or imply its endorsement, recommendation, or favoring by the United States Government or any agency thereof. The views and opinions of authors expressed herein do not necessarily state or reflect those of the United States Government or any agency thereof.

DISCLAIMER

**Portions of this document may be illegible
in electronic image products. Images are
produced from the best available original
document.**

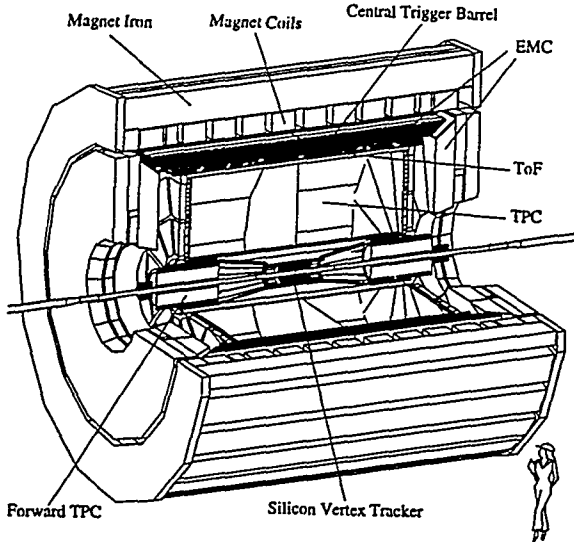


Figure 1: Cutaway view of the the STAR Detector. Major detector components are identified.

charged particles and an electromagnetic calorimeter for detecting photons and identifying electrons. Details of the various subsystems follow:

2.1 Time Projection Chambers

The primary tracking device at STAR is a large (2.2 m radius) Time Projection Chamber. The full tracking volume covers $|\eta| < 1.0$ and there is some coverage out past $|\eta| = 1.5$. Momentum resolution for fully contained tracks is given by:

$$\frac{\delta p_T}{p_T^2} \approx 0.01$$

For high rapidity tracks ($|\eta| > 1$), the resolution worsens as a function of the track's exit radius:

$$\frac{\delta p_T}{p_T^2} \approx 0.01 \times \left(\frac{R_{TPC}}{R_{\text{exit}}} \right)^2$$

The advantage of a TPC is that it is inherently a three dimensional device. By recording both the position and time of the ionization, one can convert this

to a space point. (Contrasted with MWPC's, which return a line at constant distance from the sense wire) In the environment of RHIC collisions, where there can be thousands of tracks per unit of rapidity, this is critical for pattern recognition. The disadvantage of the TPC is it's relatively long drift time: events that occur within $\approx 80 \mu\text{s}$ of each other will overlap. However, in Au-Au collisions at RHIC, collisions occur at about 1 kHz: only a few percent of events will have another event overlapping.

In addition to the position of each space point, STAR also records the amount of ionization. Since the specific ionization dE/dx is a function of a particle's velocity, combining this with the momentum measurement allows a particle's mass (and thus identity) to be determined. This technique works best when the particle's momentum is smaller than its mass.

Two smaller, radial drift TPC's will be installed in the forward and backwards regions to cover rapidities between 2.5 and 4.0.

2.2 *Silicon Vertex Tracker*

Inside of the main TPC, just outside the beampipe, is a 3-layer Silicon Vertex Tracker (SVT). Unlike most operational silicon detectors, this is a silicon drift detector: effectively a solid-state TPC. The SVT improves the momentum resolution by approximately a factor of three:

$$\frac{\delta p_T}{p_T^2} \approx 0.003$$

While a similar improvement in the momentum resolution could be applied by constraining tracks measured in the TPC to originate from the primary vertex, such a technique would fail on long lived particles such as K_s^0 's and Λ^0 's.

The position resolution of a two track vertex is 400-700 microns (for high p_T tracks), depending on the details of track kinematics and the vertexing algorithm used.

Because the ionization in silicon crystals is different than in argon gas, the addition of dE/dx information from the silicon improves particle identification over using simply the TPC.

The SVT is not planned to be installed during the Fall, 1999 run of RHIC. The risk of radiation damage is believed to be largest during the initial operation of the accelerator.

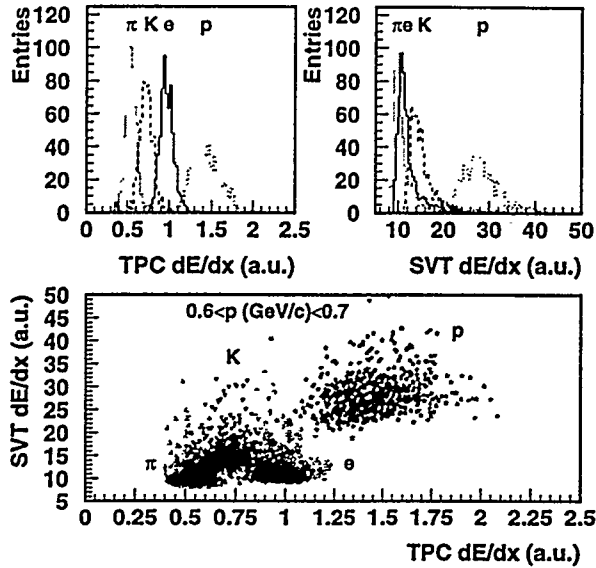


Figure 2: Ionization (dE/dx) in the TPC and SVT. Note that the separation using both measurements is better than either one by itself.

2.3 Electromagnetic Calorimeter

Outside the tracking is a lead-scintillator sampling calorimeter covering $|\eta| < 1$. This calorimeter is divided into 4800 projective towers, each 0.05×0.05 in $\eta - \phi$ space. At the depth of maximum shower development, a twin-planed wire chamber with pad readout is present to measure the shower profiles. This chamber has ten times better position resolution in each view than the towers.

The overall energy resolution of the calorimeter is specified as $20\%/\sqrt{E}$. Prototype modules have exhibited resolutions of $16\%/\sqrt{E}$ in test beams.

Approximately 10% of the calorimeter is planned to be installed for the Fall, 1999 run. Each year thereafter, approximately 30% of the full calorimeter will be added, until the calorimeter is complete.

2.4 Trigger Aspects

STAR's data acquisition can write out between 1 and 2 central Au-Au collisions per second. (Smaller events, such as peripheral Au-Au or pp collisions, can be written faster) Since at RHIC design luminosity, there are 1000 Au-Au collisions each second (including 30 "central" events), STAR needs a trigger to

select which of these events will be written to tape.

There exist on-detector and off-detector components to the trigger. Surrounding the main TPC are a set of 240 scintillator slats forming the Central Trigger Barrel. The CTB measures charged particle multiplicity in these segments of η and ϕ , via the analog pulse height of the photomultiplier output. The ability to extend the multiplicity measurement exists by reading out the primary ionization signal on the TPC amplification grid. Photons enter the trigger through the electromagnetic calorimeter, which provides fast trigger signals for $0.2 \times 0.2 \eta - \phi$ trigger towers. (Each made up of 16 detector towers.)

The trigger decision hardware exists largely off the detector. The STAR trigger is in four levels, corresponding roughly to the major time scales of the experiment: beam crossing, TPC amplification, TPC readout and event writing. For the first year of STAR operation, the earliest level of the trigger will be implemented in full, with a partial implementation of the highest level. The middle two levels exist only in a skeleton form. For the low luminosity expected in early RHIC operation, this is acceptable, but the trigger will have to grow in such a way as to match RHIC luminosity.

2.5 Possible Additions

While the baseline STAR detector is an extremely capable device, there are some enhancements that are being considered to improve on its performance. Two are the Endcap Electromagnetic Calorimeter (EEMC) and the Time of Flight array (TOF). The EEMC will extend the coverage of the calorimeter to $-1 \leq \eta \leq 2$. The TOF replaces a fraction of the CTB with finer segmented scintillator and phototubes with better timing characteristics, (70 ps) allowing us to measure the time of detection of individual particles. That information, coupled with the interaction time and position, allows us to calculate the particle's velocity, and thereby its mass. The net effect is to improve our particle identification at high transverse momentum: more details follow later in the paper.

3 Selected Physics Topics

It is of course impossible to present an exhaustive list of the physics capabilities of such a large experiment. Instead, I will discuss a few selected measurements which illustrate what STAR will be capable of.

3.1 Particle Spectra

Since STAR was designed as a hadron detector, some of the earliest measurements will be characterizing the production of these hadrons. The momentum resolution of reconstructed charged particles is (as described in detail above) $\delta p_T/p_T \approx 0.003 p_T$ (/GeV). While particle counting at the trigger level is done with the CTB, offline we count tracks found in the SVT and the TPC. Monte Carlo shows track finding efficiency above 90%, so the corrections for inefficiency are small. Accurate multiplicity counting allows us to calculate many distributions of interest: dN/dp_T , $dN/d\eta$, $d^2N/d\eta dp_T$...

While inclusive distributions are interesting in their own right, more information can be gained by measuring spectra and distributions for individual particles species. Figure 3 shows a sample distribution with and without Time of Flight.

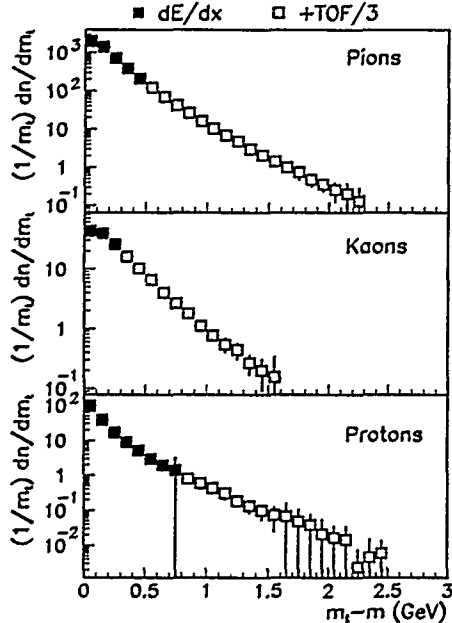


Figure 3: Monte Carlo $m_T - m$ spectrum for pions, kaons and protons with and without a patch of TOF counters installed. This particular simulation assumes 1/3 of ϕ covered by TOF.

With the addition of the EMC, STAR is not limited to looking solely at charged particles. Roughly 30% of the particles produced in a Au-Au collision are expected to be π^0 's and η 's. A detector designed for large geometric acceptance would be remiss if it let this 30% pass through undetected and unseen. With the STAR detector, individual photons can be detected down to a few hundred MeV, and the decays $\pi^0 \rightarrow \gamma\gamma$ and $\eta \rightarrow \gamma\gamma$ detected down to 1 GeV and 2-3 GeV respectively.^a The detector's upper limits on reconstruction are about 50 GeV for the π^0 and over 100 GeV for the η . The upper limit on our range is therefore limited by the production cross-section, not any instrumental effects.

One signature of a phase transition is a change in the relationship between energy and entropy in each event. Experimentally, this is accessible as a change in the relationship between average particle energy and number of particles. For charged particles, these measurements naturally follow from dN/dp_T and dN/dy . Is this sort of measurement possible with photons? After all, the calorimeter measures energy deposited in a tower, whether deposited by one or many photons. At low energies, the shower maximum detector is relatively inefficient, so using it to count photons is impractical. And, as it turns out, roughly 40% of the towers with non-zero energy have been hit by more than one photon. Fortunately, the granularity of the STAR EMC lets us measure the number of photons in another way: by counting the towers with *no* energy, we can use Poisson statistics to understand how many towers were struck by at least two photons. This technique lets us measure the average photon energy in each event to a little better than 5%.

This is important, not just as a second measurement. Statistical fluctuations cause a variation in the π^\pm/π^0 ratio event by event, and an excess or deficit of π^\pm can skew the measurement of mean pion energy. Only by looking at all three charged states can one exclude the possibility that this sort of systematic effect is faking a signal.

This discussion unfortunately ignores many other measurements we plan to undertake with reconstruction of charged and neutral hadrons: reconstructing strange baryons (Λ , Ξ , Ω^-), using interferometry to measure the particle source size, as well as other measurements.

^aIt may be possible to measure the η contribution below the threshold where we can reconstruct it by comparing the inclusive photon spectrum to what we expect from π^0 decays alone. 15-20% of the background under the π^0 peak at 1 GeV has at least one photon from $\eta \rightarrow \gamma\gamma$ decay.

3.2 Chiral Symmetry Restoration

Another new phenomenon that might be detectable at RHIC is that of Chiral Symmetry Restoration. It is suggested that pockets of matter might be formed where the isospin vector points in a different direction as in ordinary matter. As these regions cool, they can emit pions with unusual isospin ratios, and therefore unusual π^0/π^\pm ratios. As a practical matter $N(\gamma)/N(h^\pm)$ turns out to be experimentally simpler to measure than π^0/π^\pm , but the underlying physics is the same.

STAR can not only measure this quantity, but we can trigger on it, by comparing the energy in the EMC (due primarily to π^0 's) and the multiplicity in the CTB. Figure 4 shows distributions for three categories of events: normal events, events with a disoriented chiral condensate (DCC), and events with Bose-Einstein correlations included. Events with unusual EMC energy/CTB multiplicity ratios can be selected by the trigger for further analysis offline.

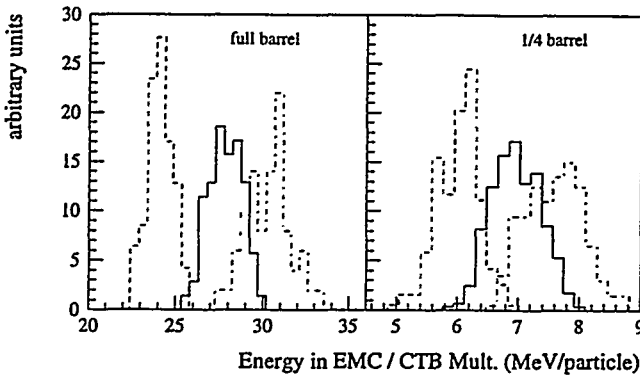


Figure 4: Ratio of EMC energy to CTB multiplicity for three classes of events: Chiral condensates (left), normal events (right) and events with Bose-Einstein correlations (right).

Discussions of DCC's often get bogged down in the question of what a realistic DCC model might look like, and whether the experiment is using an appropriate model or not. Perhaps this can be avoided by characterizing a DCC model in terms of 3 parameters:

- Its size: what area in $\eta - \phi$ space does the effect cover? Very small DCC's are hard to find, because the statistical fluctuations from only a few particles can be large.
- Its strength: in the area of interest, what is the fraction of particles that

have a different charge than what they would have in the absence of such an effect? Weak DCC's are harder to find than strong ones.

- Its cross section or frequency of occurrence. What fraction of events have a DCC? Rare events are obviously harder to find. However, in some cases, if the cross-section is too large, these events will also be hard to find. If there are many overlapping DCC's in an event, the net contributions from all of them will on average cancel, and the events look similar to each other. In this case, lower energy running of RHIC (thereby reducing the cross-section) will probably be necessary to untangle these multiple contributions.

STAR is sensitive to DCC's where the product of these three numbers is greater than 0.0015. Such DCC's would give a 3σ signal in a year of running. Obviously control over experimental systematics is an important part of such an analysis. Fortunately, there are some built-in cross checks at STAR: for example, the multiplicities as measured by the SVT, the TPC and the CTB should track each other. The multiplicities in the EMC should be independent of ϕ . And so forth. Theoretical issues may also be important.

3.3 J/ψ and Heavy Flavor Production

One signature of a Quark-Gluon Plasma that has received some recent attention is that of J/ψ suppression. In a QGP, the free color changes can screen the QCD attraction between the c and the \bar{c} . This will cause the J/ψ to "fall apart", and hadronize to open charm instead.

Interpretation of this can be complicated, because in addition to this effect, the overall production of charmed quarks can increase, due to the increase of the effective gluon flux in a plasma.

At STAR, we expect a yield of approximately 10,000 prompt $J/\psi \rightarrow e^+e^-$ events per year in central collisions. (And another 1500 or so from $b \rightarrow J/\psi X$ decays) This corresponds to an electron identification threshold of 1.5 GeV, based on test beam results.

One way of untangling the quarkonium suppression from gluon enhancement is to compare different quarkonium states with different radii (and thus suppression factors). For example, the charm quark cross section divides out in the ratio of $\sigma(\psi')/\sigma(J/\psi)$, leaving only the quarkonium suppression, expected to be larger for the ψ' . Our expected yield of ψ' mesons in the $\psi' \rightarrow e^+e^-$ channel is only about 200, over a background of several thousand. The resulting statistical uncertainty gives us at best a 30% measurement on the ratio; probably too large to be anything other than a confirming measurement. The decay $\psi' \rightarrow J/\psi \pi^+ \pi^-$ has not been investigated. The decays $\chi \rightarrow J/\psi \gamma$, $\chi \rightarrow 2\pi$ and $\chi \rightarrow 4\pi$ have all been studied, and the background rejection is

not yet good enough to incorporate them in the analysis. We expect a few dozen $\Upsilon \rightarrow e^+e^-$ events, and resolution sufficient to separate the $\Upsilon(1S)$ from the merged peaks of the $\Upsilon(2S)$ and $\Upsilon(3S)$.

The same signal for the J/ψ , high mass electron pairs, can also be used to identify open charm, via $c \rightarrow e^+X$ and $\bar{c} \rightarrow \bar{e}^-X$. Because there isn't a mass peak like the J/ψ , we will probably have to make more restrictive electron energy requirements, but even at 2 GeV, we expect a number of electron pairs from open charm comparable to the number of J/ψ 's. There will be some contamination from bottom quarks in this sample; at the present time we don't know how large this is, or if it's important: since the same gluon fusion process produces both $c\bar{c}$ and $b\bar{b}$, the impact of b contamination may be small.

It is worth pointing out that the average flight distance of a b -flavored hadron decaying to a J/ψ plus anything is 615 μm . Since this is comparable to our resolution, we can (on a statistical basis) measure the fraction of J/ψ 's from b decay. This could be used to either subtract off the b contribution to the open charm signal, or even to more directly probe J/ψ suppression. J/ψ mesons from b decay are produced microns away from the central collision, far from any plasma produced. They would therefore be unsuppressed. If prompt J/ψ mesons are suppressed, the mean flight distance of the J/ψ will increase. This technique alone gives us a 1σ sensitivity to the prompt/displaced J/ψ ratio of about 7%.

4 Conclusions

One question that I was asked at the workshop was to compare STAR and the other RHIC detectors, especially PHENIX, the other large detector. UA1 and UA2 looked rather similar; CDF and D0 look similar (and with their present upgrades are growing even more similar); BABAR and BELLE are very similar, as are SLD and the four LEP detectors: ALEPH, DELPHI, OPAL and L3. Why then do STAR and PHENIX look so different?

The answer is that at the other experiments, the signal was known (or at least predicted with strong consensus behind the predictions) in advance. That's not the case with searching for the Quark-Gluon Plasma: STAR and PHENIX have taken two different approaches on how to address this. PHENIX was designed to measure a few things very well. STAR was designed to measure many things, but not every measurement can outperform a detector specializing in that measurement. In any event, having four complementary detectors maximizes the RHIC discovery potential. STAR's particular focus on a broad spectrum of physics measurements will expand our understanding of heavy ion collisions on multiple simultaneous fronts in the very near future.